Liquid Crystals

Publication details, including instructions for authors and subscription information:
http://www.informaworld.com/smpp/title~content=t713926090

A matrix method for modelling liquid crystal textures

Tsunehisa Kimura[a]; Derek G. Gray[a]
[a] Paprican and Department of Chemistry, Pulp and Paper Research Centre, McGill University, Montreal, Canada

To cite this Article Kimura, Tsunehisa and Gray, Derek G.(1993) 'A matrix method for modelling liquid crystal textures', Liquid Crystals, 13: 1, 23 — 30

To link to this Article: DOI: 10.1080/02678299308029050

URL: http://dx.doi.org/10.1080/02678299308029050

LIQUID CRYSTALS, 1993, VOL. 13, NO. 1, 23–30

A matrix method for modelling liquid crystal textures

by TSUNEHISA KIMURA and DEREK G. GRAY*
Paprican and Department of Chemistry, Pulp and Paper Research Centre,
McGill University, Montreal, Canada H3A 2A7

(*Received 28 April 1992; accepted 17 August 1992*)

A simple method for modelling the textures of liquid-crystalline phases, recently proposed by Bedford *et al.*, is here rewritten in matrix form. A formal similarity is found between their method and the continuum theory of liquid crystals. Disclination patterns are simulated by solving a modified matrix equation.

1. Introduction

Recently, Bedford, Nicholson and Windle [1] proposed a simple lattice model for textures in liquid crystals. Using an interaction energy of the Maier–Saupe type [2, 3] between two adjacent lattice sites, with a truncation of higher terms in the Taylor expansion, they derived a simple equation determining the orientation of the director at a lattice site. They obtained disclination patterns from an initial random configuration by selecting a lattice site at random and determining the orientation of the director at the site. The process was repeated until the disclination pattern developed. Their iterative method permitted the development of disclination to be followed.

Here, we convert their equation into a matrix form and analyse the effect of periodic and fixed boundary conditions. We also derive a modified matrix equation in order to apply the matrix method to various fixed boundary conditions. A formal similarity between the method of Bedford *et al.* and the continuum theory of Frank [4] is discussed.

2. Matrix analysis of BNW model

In the two dimensional lattice model employed by Bedford *et al.* [1] (hereafter referred to as BNW), cell k, specified by the angle ϕ_k of the director to a reference direction, can interact with its four nearest neighbour cells to give the interaction energy, E_k, expressed as

$$E_k=\sum_{k'}(\phi_{k'}-\phi_k)^2, \tag{1}$$

with k' indicating a nearest neighbour. Differentiating this function with respect to ϕ_k yields

$$\phi_k=\sum_{k'}\phi_{k'}/4, \tag{2}$$

which indicates that the value ϕ_k of the centre cell is given by averaging the values of its four adjacent cells. On the other hand, the two dimensional continuum theory with the

---

* Author for correspondence.

0267–8292/93 $10·00

one constant approximation [4, 5] shows that the director field $\phi(x, y)$ satisfies the following differential equation:

$$\frac{\partial^2\phi}{\partial x^2}+\frac{\partial^2\phi}{\partial y^2}=0. \tag{3}$$

Here, $\phi\ (x, y)$ is the angle of the director to the x axis, corresponding to ϕ_k in equation (1). Applying the finite difference method [6] to equation (3), we obtain a discrete equation as follows:

$$\left.\begin{array}{l} \phi_{i-1,j}+\phi_{i+1,j}+\phi_{i,j-1}+\phi_{i,j+1}-4\phi_{ij}=0, \\ \text{or} \\ \phi_{ij}=(\phi_{i-1,j}+\phi_{i+1,j}+\phi_{i,j-1}+\phi_{i,j+1})/4, \end{array}\right\} \tag{4}$$

where i and j correspond to x and y and $i\pm1$ and $j\pm1$ correspond to the nearest neighbours of i and j, respectively. Equation (4) indicates that the value ϕ_{ij} for the centre cell is the average of the values of its four adjacent cells, $\phi_{i-1,j}$, $\phi_{i+1,j}$, $\phi_{i,j-1}$, and $\phi_{i,j+1}$. Thus, equation (4) is equivalent to equation (2). This similarity is not surprising because the energy density function derivable from BNW theory has the same functional form as that for the continuum theory (see Appendix for a comparison of the two theories in terms of energy density function). Since equation (2) holds for every cell k in a two dimensional region Ω under consideration, we obtain a set of linear equations, written in a matrix form as

$$A\phi=b, \tag{5}$$

where $\phi=\{\phi_k\}$ and $b=\{b_k\}$ $(1\leqslant k\leqslant n^2)$ are vectors and $A=\{A_{km}\}$ $(1\leqslant k, m\leqslant n^2)$ is a matrix. The values of A and b depend on the conditions imposed at the boundary of the region Ω. n^2 is the total number of cells in the system.

Now we examine equation (5) using a simple system with 4 × 4 cells shown in figure 1. For a system with a periodic boundary condition, equation (5) is written as

$$A_{\mathrm{p}}\phi=0, \tag{6}$$

with A_{p} given in the table. Here, the constant term b in equation (5) vanishes. Since the equation dealing with a boundary, say ϕ_2 in figure 1, is written as $\phi_1+\phi_3+\phi_6+\phi_{14}$

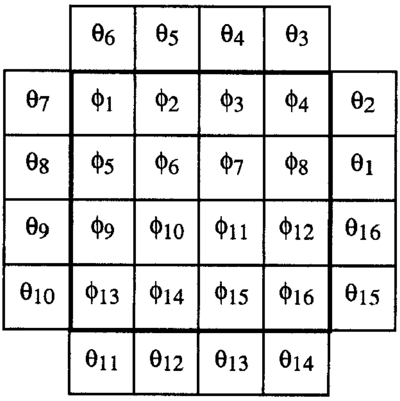

	θ_6	θ_5	θ_4	θ_3	
θ_7	ϕ_1	ϕ_2	ϕ_3	ϕ_4	θ_2
θ_8	ϕ_5	ϕ_6	ϕ_7	ϕ_8	θ_1
θ_9	ϕ_9	ϕ_{10}	ϕ_{11}	ϕ_{12}	θ_{16}
θ_{10}	ϕ_{13}	ϕ_{14}	ϕ_{15}	ϕ_{16}	θ_{15}
	θ_{11}	θ_{12}	θ_{13}	θ_{14}	

Figure 1. Assignment of ϕ_i and boundary value θ_i for the system with $n=4$.

$-4\phi_2=0$, no constant term appears in equation (6). A numerical analysis of A_p using the singular value decomposition (SVD) method [6] shows that the rank of A_p is 15 ($=n^2-1$) and the solution of equation (6) is given by

$$\phi_1=\phi_2=\ldots=\phi_{16}=\text{constant}, \tag{7}$$

indicating that the only conformation permitted to the system with a periodic boundary condition is that with uniform orientation. On the other hand, for the system with a fixed boundary condition, equation (5) is written as

$$A_\mathrm{f}\phi=b, \tag{8}$$

with A_f and b given in the table. Here, the constant term b in quation (5) does not vanish. Since the equation dealing with a boundary, say ϕ_2 in figure 1, is written as $\phi_1+\phi_3+\phi_6-4\phi_2=-\theta_5$, a constant term, $-\theta_5$, appears in equation (8). Numerical analysis of A_f using the SVD method shows that the rank of A_f is 16 ($=n^2$), hence the inverse matrix exists and the solution of equation (8) is given by

$$\phi=A_\mathrm{f}^{-1}b, \tag{9}$$

where A_f^{-1} is the inverse of A_f. The SVD analysis for systems with $n=2$, 3, 5, and 6 shows that the same tendency as for $n=4$ holds for these values of n, i.e. the rank of matrix A is n^2-1 for the periodic boundary condition and n^2 for the fixed boundary condition, and the solution for the former condition is given by $\phi_1=\phi_2=\ldots=\phi_\mathrm{n}^2=\text{constant}$, while that for the latter condition is given by $\phi=A_\mathrm{f}^{-1}b$. The same trend is expected for larger systems.

Extension of the matrix method to three dimensions is not trivial, due to the non-linear nature of the three dimensional analogue to equation (4).

3. Alternative matrix method

In this section, we derive an alternative to equation (8) in order to apply the matrix method to systems with boundary conditions that are selected to encourage the formation of disclinations. For a two dimensional region containing a disclination, the boundary value of θ_i (see figure 1) changes by $2\pi s$ with one single turn around the boundary; here, s is the strength of the disclination and has an integer or a half integer value. As a result, a jump of $2\pi s$ takes place on the boundary. The jump has no physical meaning because $\phi+2\pi s$ is equivalent to ϕ. Thus, equation (8) does not work appropriately, and requires some modification.

For this purpose, we go back to the original equation of BNW,

$$E_k=\sum_{k'}\sin^2(\phi_{k'}-\phi_k), \tag{10}$$

and the condition $\partial E_k/\partial\phi_k=0$:

$$\sin 2\phi_k/\cos 2\phi_k=\left(\sum_{k'}\sin 2\phi_{k'}\right)\bigg/\left(\sum_{k'}\cos 2\phi_{k'}\right), \tag{11}$$

from which equations (1) and (2) were derived for small $\phi_{k'}-\phi_k$ values, respectively. Rewriting equation (11) as

$$\sin 2\phi_k=\alpha\sum_{k'}\sin 2\phi_{k'} \quad\text{and}\quad \cos 2\phi_k=\alpha\sum_{k'}\cos 2\phi_{k'} \tag{12}$$

Matrix A_p for periodic boundary condition and matrix A_f and b for fixed boundary condition.

$$A_p=\begin{pmatrix}
-4 & 1 & 0 & 1 & 1 & 0 & 0 & 0 & 0 & 0 & 0 & 0 & 1 & 0 & 0 & 0\\
1 & -4 & 1 & 0 & 0 & 1 & 0 & 0 & 0 & 0 & 0 & 0 & 0 & 1 & 0 & 0\\
0 & 1 & -4 & 1 & 0 & 0 & 1 & 0 & 0 & 0 & 0 & 0 & 0 & 0 & 1 & 0\\
1 & 0 & 1 & -4 & 0 & 0 & 0 & 1 & 0 & 0 & 0 & 0 & 0 & 0 & 0 & 1\\
1 & 0 & 0 & 0 & -4 & 1 & 0 & 1 & 1 & 0 & 0 & 0 & 0 & 0 & 0 & 0\\
0 & 1 & 0 & 0 & 1 & -4 & 1 & 0 & 0 & 1 & 0 & 0 & 0 & 0 & 0 & 0\\
0 & 0 & 1 & 0 & 0 & 1 & -4 & 1 & 0 & 0 & 1 & 0 & 0 & 0 & 0 & 0\\
0 & 0 & 0 & 1 & 1 & 0 & 1 & -4 & 0 & 0 & 0 & 1 & 0 & 0 & 0 & 0\\
0 & 0 & 0 & 0 & 1 & 0 & 0 & 0 & -4 & 1 & 0 & 1 & 1 & 0 & 0 & 0\\
0 & 0 & 0 & 0 & 0 & 1 & 0 & 0 & 1 & -4 & 1 & 0 & 0 & 1 & 0 & 0\\
0 & 0 & 0 & 0 & 0 & 0 & 1 & 0 & 0 & 1 & -4 & 1 & 0 & 0 & 1 & 0\\
0 & 0 & 0 & 0 & 0 & 0 & 0 & 1 & 1 & 0 & 1 & -4 & 0 & 0 & 0 & 1\\
1 & 0 & 0 & 0 & 0 & 0 & 0 & 0 & 1 & 0 & 0 & 0 & -4 & 1 & 0 & 1\\
0 & 1 & 0 & 0 & 0 & 0 & 0 & 0 & 0 & 1 & 0 & 0 & 1 & -4 & 1 & 0\\
0 & 0 & 1 & 0 & 0 & 0 & 0 & 0 & 0 & 0 & 1 & 0 & 0 & 1 & -4 & 1\\
0 & 0 & 0 & 1 & 0 & 0 & 0 & 0 & 0 & 0 & 0 & 1 & 1 & 0 & 1 & -4
\end{pmatrix}$$

$$A_f=\begin{pmatrix}
-4 & 1 & 0 & 0 & 1 & 0 & 0 & 0 & 0 & 0 & 0 & 0 & 0 & 0 & 0 & 0\\
1 & -4 & 1 & 0 & 0 & 1 & 0 & 0 & 0 & 0 & 0 & 0 & 0 & 0 & 0 & 0\\
0 & 1 & -4 & 1 & 0 & 0 & 1 & 0 & 0 & 0 & 0 & 0 & 0 & 0 & 0 & 0\\
0 & 0 & 1 & -4 & 0 & 0 & 0 & 1 & 0 & 0 & 0 & 0 & 0 & 0 & 0 & 0\\
1 & 0 & 0 & 0 & -4 & 1 & 0 & 0 & 1 & 0 & 0 & 0 & 0 & 0 & 0 & 0\\
0 & 1 & 0 & 0 & 1 & -4 & 1 & 0 & 0 & 1 & 0 & 0 & 0 & 0 & 0 & 0\\
0 & 0 & 1 & 0 & 0 & 1 & -4 & 1 & 0 & 0 & 1 & 0 & 0 & 0 & 0 & 0\\
0 & 0 & 0 & 1 & 0 & 0 & 1 & -4 & 0 & 0 & 0 & 1 & 0 & 0 & 0 & 0\\
0 & 0 & 0 & 0 & 1 & 0 & 0 & 0 & -4 & 1 & 0 & 0 & 1 & 0 & 0 & 0\\
0 & 0 & 0 & 0 & 0 & 1 & 0 & 0 & 1 & -4 & 1 & 0 & 0 & 1 & 0 & 0\\
0 & 0 & 0 & 0 & 0 & 0 & 1 & 0 & 0 & 1 & -4 & 1 & 0 & 0 & 1 & 0\\
0 & 0 & 0 & 0 & 0 & 0 & 0 & 1 & 0 & 0 & 1 & -4 & 0 & 0 & 0 & 1\\
0 & 0 & 0 & 0 & 0 & 0 & 0 & 0 & 1 & 0 & 0 & 0 & -4 & 1 & 0 & 0\\
0 & 0 & 0 & 0 & 0 & 0 & 0 & 0 & 0 & 1 & 0 & 0 & 1 & -4 & 1 & 0\\
0 & 0 & 0 & 0 & 0 & 0 & 0 & 0 & 0 & 0 & 1 & 0 & 0 & 1 & -4 & 1\\
0 & 0 & 0 & 0 & 0 & 0 & 0 & 0 & 0 & 0 & 0 & 1 & 0 & 0 & 1 & -4
\end{pmatrix}
\quad
b=\begin{pmatrix}
-\theta_6-\theta_7\\
-\theta_5\\
-\theta_4\\
-\theta_2-\theta_3\\
-\theta_8\\
0\\
0\\
-\theta_1\\
-\theta_9\\
0\\
0\\
-\theta_{16}\\
-\theta_{10}-\theta_{11}\\
-\theta_{12}\\
-\theta_{13}\\
-\theta_{14}-\theta_{15}
\end{pmatrix}$$

and putting $\alpha=1/4$ as an approximation, we obtain a set of equations for $\cos 2\phi_k$ and $\sin 2\phi_k$ similar to equation (2). Equation (12) can be readily transformed into matrix forms as

$$A_f\mathbf{S}=b_s \quad \text{and} \quad A_f\mathbf{C}=b_c, \tag{13}$$

where the elements of vectors $\mathbf{S}$ and $\mathbf{C}$ are defined as

$$\mathbf{S}_k=\sin 2\phi_k \quad \text{and} \quad \mathbf{C}_k=\cos 2\phi_k. \tag{14}$$

The elements of b_s and b_c are calculated in the same way as in the table by replacing θ_i with $\cos 2\theta_i$ and $\sin 2\theta_i$, respectively. A_f is the same as in equation (8). After the two matrix equations in equation (13) are solved, ϕ_k is determined by

$$\tan 2\phi_k=\mathbf{S}_k/\mathbf{C}_k \tag{15}$$

for each k. Here, we notice that equation (15) is the condition for minimum as well as maximum; the equation has four solutions, two for minima, ϕ and $\phi+\pi$, and the others for maxima, $\phi+\pi/2$ and $\phi+3\pi/2$. Therefore, the orientation with minimum energy for

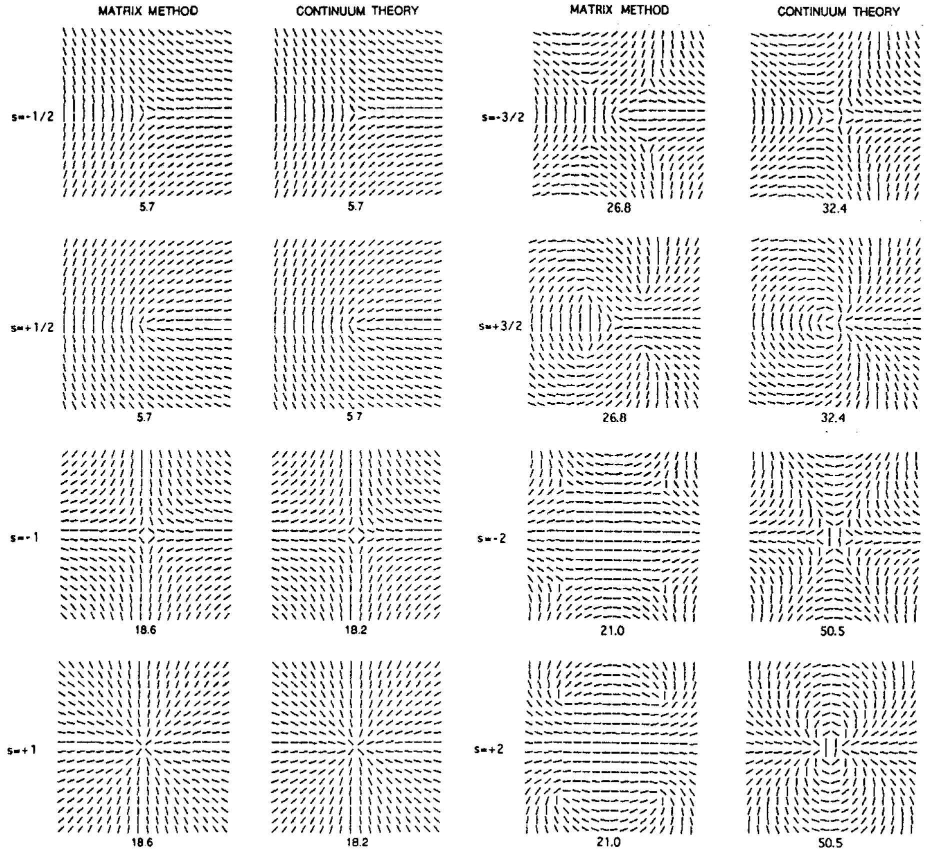

Figure 2. Disclination patterns obtained by matrix method (left) and continuum theory (right) for various s values. The number below each pattern indicates the total energy (E_{tot}).

each cell can be determined by the following procedure. First, we pick up one of the outermost cells, ϕ_k, which is in contact with a boundary cell θ_i. Since θ_i is given, we can choose one of the solutions for ϕ_k from equation (15) so as to minimize the interaction between θ_i and ϕ_k. Index k runs over all the outermost cells having contact with the boundary cells. The same procedure is repeated, moving inwards to the next layer of cells, using the ϕ_k values determined in the previous step until the procedure arrives at the core of the system. After completion of the above process, the first and the second derivatives of E_k (see equation (10)) are calculated for each k to confirm the minimum; a vanishing first derivative with a positive second derivative indicates the minimum.

Figure 2 shows the disclination patterns obtained for the boundary conditions encouraging $s = \pm 1/2$, ± 1, $\pm 3/2$, and ± 2 disclination in the centre. Also, disclination patterns calculated by the continuum theory [4, 7],

$$\phi = s\Psi, \quad \tan\Psi = y/x, \tag{16}$$

are shown for comparison. The root mean square errors estimated by

$$\sigma = \sqrt{\left(\frac{1}{n^2}\sum_k\left[\phi_k - \tfrac{1}{2}\tan^{-1}\left\{\left(\sum_{k'}\sin 2\phi_{k'}\right)\Big/\left(\sum_{k'}\cos 2\phi_{k'}\right)\right\}\right]^2\right)}, \tag{17}$$

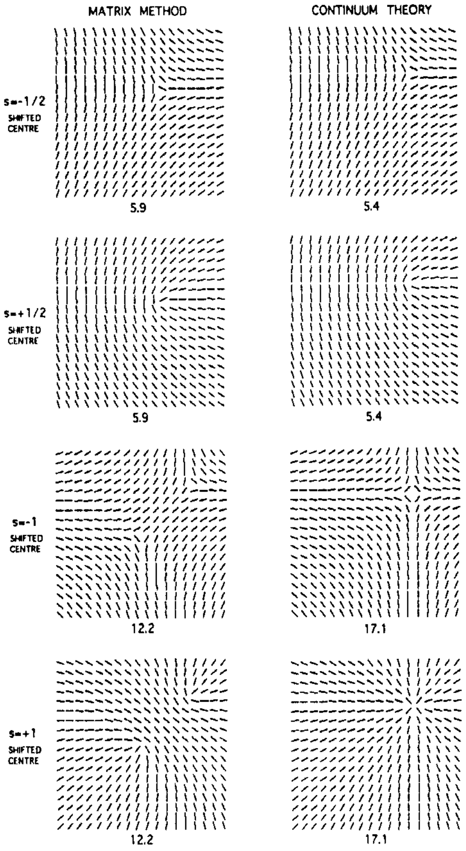

Figure 3. Disclination patterns obtained by matrix method (left) and continuum theory (right) for $s=\pm 1/2$ and ± 1 with a decentralizing boundary condition. The number below each pattern indicates the total energy (E_{tot}).

are 0·2, 1·1, 1·9, and 0·7° for patterns by the matrix method and 0·2, 0·7, 2·8 and 4·8° for patterns by the continuum theory. A large σ value of 2·8 and 4·8° for $s=\pm 3/2$ and ± 2 in case of the continuum theory is mainly due to some central cells. A comparison of the two sets of σ indicates that the accuracy of the numerical calculation is satisfactory.

In the case of $|s| \geqslant 3/2$, the patterns obtained by the matrix method do not reproduce the patterns calculated by the continuum theory. Complicated disclination patterns in the cores, observed for the continuum theory, are split into a number of $s=\pm 1/2$ type patterns. On the other hand, a splitting does not occur for $s=\pm 1$. In this case, the procedure for determining the minimum orientation with respect to an outer cell does not work because the four core cells show negative second derivatives. The failure of the procedure might be attributed to the higher symmetry in the boundary conditions combined with the symmetry inherent in the procedure. In fact, as seen from figure 3, a similar splitting is also observed even for $s=\pm 1$, in those cases where a boundary condition is selected to encourage the generation of disclinations that are shifted away from the centre of the system (decentralizing boundary conditions); $s=\pm 1$ disclinations tend to be converted to $s=\pm 1/2$ disclinations. Disclination patterns for $s=\pm 1/2$ are stable for the decentralizing boundary condition (see figure 3).

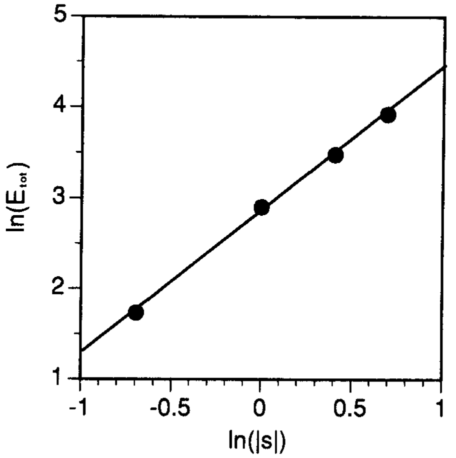

Figure 4. Logarithmic plot of total energy (E_{tot}) against the absolute value of the strength of disclination, $|s|$, obtained for the continuum theory with $n=18$.

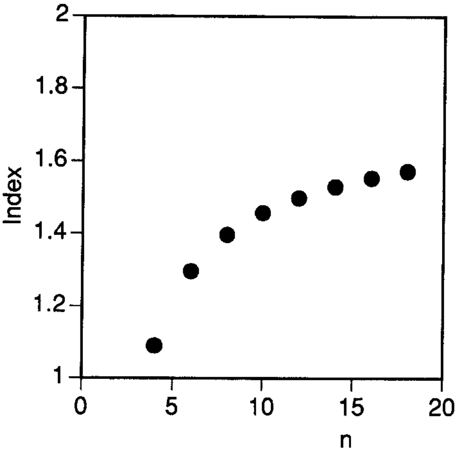

Figure 5. Effect of lattice size (n) on the index for the continuum theory.

The above observation might be explained in terms of the total energies of the systems shown in figures 2 and 3, evaluated by means of the following equation:

$$E_{\text{tot}}=\frac{1}{2}\sum_{k}\sum_{k'}\sin^2(\phi_{k'}-\phi_k). \tag{18}$$

A comparison of the total energies for the patterns obtained by the matrix method and by the continuum theory shows that for systems with $|s|\geqslant 3/2$, the total energy of the former is always smaller than the latter. This indicates that systems with a disclination of higher strength tend to create a couple of disclinations of lower strength in order to lower their total energy [8, 9].

In figure 4, a logarithmic plot of the total energy E_{tot} against $|s|$ is shown for the patterns obtained for the continuum theory. We find

$$E_{\text{tot}}=|s|^{1\cdot 57}, \tag{19}$$

where the index of 1·57 is smaller than the theoretical value of 2 [5]. The discrepancy might be partially attributed to the underestimation of the core energy, especially for large $|s|$, due to the discrete modelling employed here. In fact, the core is represented by only four cells which are insufficient to describe the continuous situation: For $s=\pm 2$, for example, four core cells even take a parallel alignment, forming a low energy core. In figure 5, the effect of lattice size on the index is shown. The index increases gradullly with increasing lattice size from 4 to 18 (the lattice size in figures 2 and 3). The asymptotic value seems slightly larger than 1·57.

We thank the Natural Sciences and Engineering Research Council of Canada for support.

Appendix

Following Vertogen [10], we write the energy density function at site **r** in two dimension as follows:

$$E(\mathbf{r})=\int\!\!\int J(\mathbf{r}')(\phi(\mathbf{r}+\mathbf{r}')-\phi(\mathbf{r}))^2\,d\mathbf{r}',$$

where ϕ is the director angle to a reference direction, and $J(\mathbf{r}')$ is a function of the distance $\mathbf{r}'$ between two directors $\phi(\mathbf{r}+\mathbf{r}')$ and $\phi(\mathbf{r})$. We expand the term of the difference of two angles with respect to $\mathbf{r}'$ and truncate higher terms because $J(\mathbf{r}')$ is a rapidly decreasing function of $\mathbf{r}'$ to obtain:

$$\phi(\mathbf{r}+\mathbf{r}')-\phi(\mathbf{r})=(\nabla\phi)\cdot\mathbf{r}'.$$

Approximating the above term by its maximum value, we obtain

$$\begin{aligned}E(\mathbf{r})&\cong\int\!\!\int J(\mathbf{r}')\mathbf{r}'^2(\nabla\phi)^2 d\mathbf{r}'\\&=\left[\int\!\!\int J(\mathbf{r}')r'^2 d\mathbf{r}'\right](\nabla\phi)^2.\end{aligned}$$

This is compared to the energy density function in the continuum theory with elastic constant K [5],

$$F_d=\frac{K}{2}(\nabla\phi)^2,$$

from which equation (3) is derived.

References

[1] Bedford, S. E., Nicholson, T. M., and Windle, A. H., 1991, *Liq. Crystals*, **10,** 63.

[2] Maier, W., and Saupe, A., 1959, *Z. Naturf.* (*a*), **14,** 882; 1960, *Ibid.*, **15,** 287.

[3] Denham, J. H., Luckhurst, G. R., Zannoni, C., and Lewis, J. W., 1980, *Molec. Crystals liq. Crystals*, **60,** 185.

[4] Frank, F. C., 1958, *Discuss. Faraday Soc.*, **25,** 1.

[5] de Gennes, P. G., 1974, *The Physics of Liquid Crystals* (Clarendon Press).

[6] Press, W. H., Flannery, B. P., Teukolsky, S. A., and Vetterling, W. T., 1989, *Numerical Recipes* (Cambridge University Press).

[7] Friedel, G., 1922, *Annales. Phys.*, **19,** 273.

[8] Brezis, H., 1989, *Theory and Applications of Liquid Crystals*, edited by J. L. Ericksen and D. Kinderlehrer (Springer-Verlag), p. 31.

[9] Cohen, R., and Hardt, R., 1989, *Theory and Applications of Liquid Crystals*, edited by J. L. Ericksen and D. Kinderlehrer (Springer-Verlag), p. 99.

[10] Vertogen, G., 1983, *Physica* A, **117,** 227.